On the resonances and polarizabilities of split ring resonators

J. García-García[a] and F. Martín[b]
Department d'Enginyeria Electrònica, Universitat Autònoma de Barcelona, 08193 Bellaterra, Barcelona, Spain

J. D. Baena and R. Marqués[c]
Departamento de Electrónica y Eletromagnetismo, Facultad de Física, Universidad de Sevilla, Avenida Reina Mercedes s/n, 41012 Sevilla, Spain

L. Jelinek[d]
Department of Electromagnetic Field, Czech Technical University in Prague, Technicka 2, 16627, Praha 6, Czech Republic

(Received 8 February 2005; accepted 29 June 2005; published online 10 August 2005)

In this paper, the behavior at resonance of split ring resonators (SRRs) and other related topologies, such as the nonbianisotropic SRR and the broadside-coupled SRR, are studied. It is shown that these structures exhibit a fundamental resonant mode (the quasistatic resonance) and other higher-order modes which are related to dynamic processes. The excitation of these modes by means of a properly polarized time varying magnetic and/or electric fields is discussed on the basis of resonator symmetries. To verify the electromagnetic properties of these resonators, simulations based on resonance excitation by nonuniform and uniform external fields have been performed. Inspection of the currents at resonances, inferred from particle symmetries and full-wave electromagnetic simulations, allows us to predict the first-order dipolar moments induced at the different resonators and to develop a classification of the resonances based on this concept. The experimental data, obtained in SRR-loaded waveguides, are in agreement with the theory and point out the rich phenomenology associated with these planar resonant structures. © *2005 American Institute of Physics*. [DOI: 10.1063/1.2006224]

I. INTRODUCTION

In the recent years, split ring resonators (SRRs), originally proposed by Pendry *et al.*[1] [see Fig. 1(a)], have attracted a great interest among electromagneticians and microwave engineers, due to their applications in the synthesis of artificial materials (metamaterials) with negative effective permeability μ based on periodic arrangements of these resonators.[1,2] This can be achieved in a certain frequency range (i.e., in a narrow frequency band above the resonant frequency of SRRs, f_0) and for incident radiation of the appropriate polarization (namely, magnetic-field vector applied parallel to the ring axis). The key to this success in the generation of such artificial media is the fact that, in the vicinity of resonance, SRR dimensions are small as compared to signal wavelength. Therefore, an array composed of these constitutive particles can be considered as an effective (continuous) medium with effective electromagnetic parameters, which can be deduced from the polarizabilities of these particles when they are illuminated by an external uniform field of the appropriate polarization.[1] The synthesis of a material with negative magnetic permeability was carried out by Smith *et al.*, at the University of California—San Diego (UCSD).[2] They fabricated a bulk structure composed of several rows of SRRs printed on dielectric slabs. It is worth mentioning at this point that the group of Smith also provided experimental evidence of left-handed wave propagation,[2] something studied by Veselago[3] in the late 1960s, but considered as theoretical speculation during those years. The synthesis of negative permeability media by means of SRRs opened the door to the design of metamaterials that are able to exhibit left-handed wave propagation and negative refractive index in a certain frequency region of the electromagnetic spectrum.[2,4] After these seminal works, several left-handed metamaterials based on SRRs in one-dimensional (1D) configurations were reported, including waveguide[5,6] and planar technologies,[7] thus pointing out the significance of these subwavelength resonators and their potentiality, not only to verify the exotic electromagnetic properties of left-handed metamaterials predicted by Veselago, but also to design functional microwave devices with improved performance and reduced dimensions.[8]

As it was already mentioned, the continuous medium parameters describing the aforementioned SRR arrays can be predicted from their individual electromagnetic behavior near the resonances. The behavior of SRRs at the first resonance is well known. As it was reported in Ref. 9, the application of an axial, uniform, and time varying magnetic field to the rings induces current loops at resonance. These current loops are closed through the distributed (edge) capacitance between concentric rings (which can be potentially very high due to the presence of the splits) and the particle behaves as an externally driven *LC* resonator. On account of the current circulation between rings and the relatively large value of the

[a]Electronic mail: joan.garcia@uab.es
[b]FAX: 34 93 581 26 00; electronic mail: ferran.martin@uab.es
[c]Electronic mail: marques@us.es
[d]Electronic mail: bish@atlas.cz

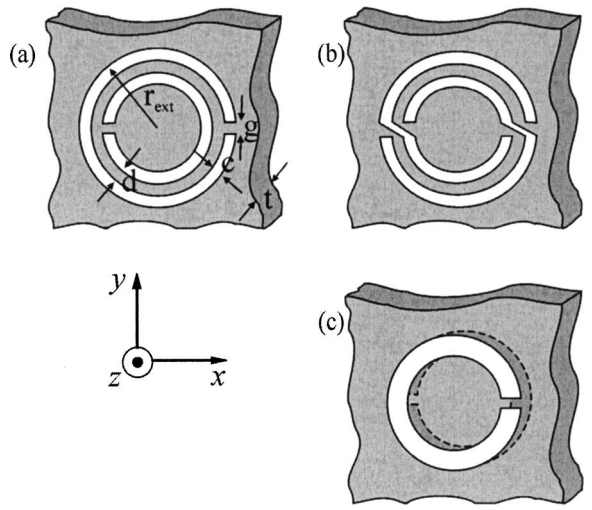

FIG. 1. Topologies for the EC-SRR (a), NB-SRR (b), BC-SRR (c), and relevant dimensions. The gray zones represent the dielectric substrate and the white zones the metallization.

edge capacitance achievable, the electrical size of the particle can be made small at resonance, this being a key aspect of SRRs, in comparison with conventional single-ring resonators. This means that SRRs can be considered as lumped or quasilumped elements. However, if the slits are removed (i.e., closed rings), no significant current flows between the inner and outer rings, and the behavior of the structure is no longer controlled by the distributed capacitance between concentric rings, as has been verified by electromagnetic simulations (not shown) of closed ring pairs excited by means of a microstrip transmission line (see Sec. III). Current loops can also be induced by a uniform time varying electric field lying in the particle plane[9–11] and oriented in the orthogonal direction to the imaginary line connecting the slits (y axis in Fig. 1). This is due to the dipolar electric moment induced in the rings, as a consequence of the cross-polarization effects present in the SRR first resonance. Similarly, a magnetic field applied in the axial direction is also able to induce this dipolar electric moment.[11] This bianisotropic behavior of SRRs is closely related to their topology, as it will be shown later. On the basis of the above concepts, other resonant particles have been proposed in order to avoid or enhance some SRR properties. Thus, a broadside-coupled SRR (BC-SRR) configuration [see Fig. 1(c)] was proposed in Ref. 9 in order to avoid cross-polarization effects, as well as to further reduce the electrical size of the SRR at resonance. Besides, it is possible to avoid cross-polarization effects while keeping the single-plane geometry of the SRR.[12] One of the resulting particles is the so-called nonbianisotropic SRR (NB-SRR), depicted in Fig. 1(b).

As it was already mentioned, for conventional SRRs [from now on edge-coupled SRR (EC-SRR) to clearly distinguish them from the other cited particles], NB-SRRs, and BC-SRRs, the electromagnetic behavior in the vicinity of their quasistatic (first) resonance is well understood (as described in Ref. 9, the term quasistatic resonance obeys to the quasistatic analysis carried out on the particle on account of its small electrical size at this frequency). However, these particles present many other resonances (higher-order resonances), which are related to dynamic processes. Indeed, for the complete characterization of artificial media and other devices made by arraying SRRs, a complete knowledge of all the resonances and polarizabilities of its constituents is necessary. Although some efforts have been made in these directions,[13,14] there still remain many open questions, and our knowledge of SRR resonances is far from being complete. To further advance in this knowledge, giving an overview of the behavior of SRRs (and derived geometries) at its different resonances, is the main goal of this paper. It will be organized as follows: in Sec. II the symmetries of the SRRs are analyzed and some basic properties of their resonances are extracted. In Sec. III the diagrams of surface current distributions for the analyzed resonances are obtained from frequency-domain full-wave simulations in a microstrip line environment. The study of these currents validates the previous theoretical analysis, also being the starting point for conclusions. In Sec. IV experiments and simulations in a waveguide environment are presented. From this study, the main features of the SRR polarizabilities in its two first resonances are extracted and compared with those deduced from symmetry considerations. Finally, the main conclusions of the work will be highlighted in Sec. V.

II. RESONANCE SYMMETRIES AND POLARIZABILITIES

The three SRRs shown in Fig. 1 can be seen as two strongly coupled rings. These rings are identical (only orientation vary) for the NB-SRR and the BC-SRR [Figs. 1(b) and 1(c)]. Therefore, it is expected that the frequencies of resonance of these particles will appear as a consequence of the splitting of the frequencies of resonance of its constitutive single rings, i.e., one above and other below. Therefore, the number of resonances in a given frequency interval for the NB- and BC-SRR should be approximately twice the number of resonances of its constituent single rings in such interval. The resonances of each single ring appear approximately at those frequencies where its mean perimeter (in the following we will apply indistinctly the denomination SRR to anyone of the resonators shown in Fig. 1) is about an integer number of half the wavelength (which is different than the free space half wavelength since the rings are etched on a dielectric slab). The slight deviation from the half-wavelength condition is due to the slit capacitance, which introduces a certain phase shift in the reflected waves. According to the previous comments, it can be deduced that two frequencies of resonance for the SRRs will appear around these frequencies. The only exception to this rule is the first resonance, which is well known to be of quasistatic nature,[9,12,13] and it can appear well below the first single-ring resonance. It can be easily deduced from the analyses in Refs. 12 and 13 that these first resonances show a distribution of currents on the rings which is antisymmetric, in the sense that the surface current on a given point of a ring, namely, the ring A, $\boldsymbol{J}_{s,A}(x,y)$, has the same amplitude but opposite sign than the surface current on the other ring, namely, the ring B, at the point $(-x,-y)$: $\boldsymbol{J}_{s,A}(x,y)=-\boldsymbol{J}_{s,B}(-x,-y)$. In fact, this property is a consequence of the inversion symmetry of the NB-SRR

and the BC-SRR (with regard to its center), and can be extended to the higher-order resonances, which can be classified as *symmetric* [those showing the property $\boldsymbol{J}_{s,A}(x,y)=\boldsymbol{J}_{s,B}(-x,-y)$] and *antisymmetric* [those retaining the above property $\boldsymbol{J}_{s,A}(x,y)=-\boldsymbol{J}_{s,B}(-x,-y)$]. Thus, it is expected that each single-ring resonance will split into two SRR resonances, one symmetric and other antisymmetric. It follows directly from this classification (and from the definitions of the electric and magnetic dipolar moments) that the symmetric resonances cannot produce any magnetic dipolar moment, whereas the antisymmetric ones, which should have a symmetric charge distribution, cannot produce any electric dipolar moment. A particular case of this last property is the well-known behavior of the first (quasistatic and antisymmetric) resonance for the considered NB-SRR and BC-SRR; it is essentially a magnetic resonance, which do not present cross-polarization effects.[9,12,13]

The onset of the resonances for the conventional EC-SRR [Fig. 1(a)] is expected to be slightly different. Since both rings forming the particle are not identical, its individual frequencies of resonance must be different. Therefore, when they are strongly coupled to form an EC-SRR, its frequencies of resonance will change as a consequence of that coupling. Thus, the final number of these resonances in a given frequency interval will remain constant, i.e., it will be roughly the same as for the system of two uncoupled rings. The stronger the coupling, the wider the difference between the EC-SRR resonances and those of its constituent rings. From the above considerations it directly follows that the classification in symmetric and antisymmetric does not hold for the EC-SRR resonances. Thus, bianisotropic effects could be present in this particle, as it actually occurs.[9,13]

It is well known that the radiation properties of small particles are mainly determined by its first-order (dipolar) electric and magnetic moments. Therefore, the analysis of the resonant dipolar moments generated at these resonances is of interest in our study. Since all the studied SRRs are planar structures, with the currents confined to a plane (the *x*-*y* plane in Fig. 1), only three types of dipolar moments can be generated: m_z (magnetic moment perpendicular to the particle plane), and p_x and p_y (electric moments in the particle plane). Thus, when the particles are illuminated by an external and uniform (at the particle scale) time-harmonic electromagnetic field, only the six independent resonant polarizabilities $\alpha_{xx}^{\ ee}$, $\alpha_{yy}^{\ ee}$, $\alpha_{zz}^{\ mm}$, $\alpha_{xy}^{\ ee}$, $\alpha_{xz}^{\ em}$, and $\alpha_{yz}^{\ em}$ (referred to the coordinate system shown in Fig. 1) arise, giving the general polarizability tensor:

$$p_x = \alpha_{xx}^{\ ee}E_x + \alpha_{xy}^{\ ee}E_y + \alpha_{xz}^{\ em}B_z, \tag{1a}$$

$$p_y = \alpha_{xy}^{\ ee}E_x + \alpha_{yy}^{\ ee}E_y + \alpha_{yz}^{\ em}B_z, \tag{1b}$$

$$m_z = -\alpha_{xz}^{\ em}E_x - \alpha_{yz}^{\ em}E_y + \alpha_{zz}^{\ mm}B_z, \tag{1c}$$

where the symmetry properties for the polarizabilities coming from Onsager relations have been implicitly introduced.[15] For lossless SRRs, the polarizability tensor must be Hermitian, thus $\alpha_{xx}^{\ ee}$, $\alpha_{yy}^{\ ee}$, $\alpha_{zz}^{\ mm}$, and $\alpha_{xy}^{\ ee}$ must be real, and $\alpha_{yz}^{\ em}$ and $\alpha_{xz}^{\ em}$ imaginary.

It has been already shown that the bianisotropic polarizabilities $\alpha_{yz}^{\ em}$ and $\alpha_{xz}^{\ em}$ vanish for all resonances of the NB-SRR and the BC-SRR (this fact can be also deduced from the inversion symmetry of these configurations, and from the transformation properties of the electric and magnetic quantities by this symmetry). There still remains another possible cross-polarization term in (1), the $\alpha_{xy}^{\ ee}$ polarizability. However, since the electric polarizability tensor in the *x*-*y* plane is symmetric, it is always possible to find a coordinate system for which this tensor diagonalizes. It can be easily shown that this system is that adopted in Fig. 1 for the EC-SRR and the BC-SRR [Figs. 1(a) and 1(c)]. In fact, these configurations present symmetry by reflection at the *z*-*x* plane. Therefore, if a dipole p_y would be generated when one of these SRRs is illuminated by an electric field E_x, from the aforementioned symmetry it follows that the opposite dipole should be also generated, which is clearly impossible. Regarding to the NB-SRR, this last property cannot be shown. However, since this configuration presents a *high degree* of the aforementioned reflection symmetry, it can be expected that $\alpha_{xy}^{\ ee}\approx 0$. Returning now to the EC-SRR, the cross polarizabilities $\alpha_{yz}^{\ em}$ and $\alpha_{xz}^{\ em}$ will not vanish, in general. However, from the reflection symmetry of this configuration with regard to the *z*-*x* plane (and from the transformation properties of the electric and magnetic quantities by this symmetry) it directly follows that $\alpha_{xz}^{\ em}=0$. In summary, for the BC-SRR we should have $\alpha_{xy}^{\ ee}=\alpha_{xz}^{\ em}=\alpha_{yz}^{\ em}=0$; for the NB-SRR $\alpha_{xz}^{\ em}=\alpha_{yz}^{\ em}=0$ and $\alpha_{xy}^{\ ee}\approx 0$; and for the EC-SRR $\alpha_{xy}^{\ ee}=\alpha_{xz}^{\ em}=0$. These symmetries are valid for all the resonances of the aforementioned configurations. For specific resonances, additional symmetries may occur as a consequence of the specific symmetry of this resonance. For instance, it has been already mentioned that, in symmetric resonances, all the magnetic polarizabilities must vanish: $\alpha_{zz}^{\ mm}=\alpha_{xz}^{\ em}=\alpha_{yz}^{\ mm}=0$.

III. SURFACE CURRENT DISTRIBUTION IN SRR RESONANCES

It is well known that the field and/or current distribution in a resonator, near one of its resonances, does not significantly depend on the excitation. Thus, in principle, any excitation can be used to study the current distribution at SRR resonances. Since it is expected, from the above considerations, that uniform fields only will excite a subset of the SRR resonances, excitation by a strongly nonuniform field would be preferable if one wants to excite all SRR resonances in a single experiment. To this end, the microstrip excitation procedure reported in Ref. 16, where the SRR is capacitively and inductively coupled to the microstrip, seems to fulfill all the requirements. In fact, the structure shown in Fig. 2 has been used to find the SRR resonances (by simulation of its transmission coefficients) and to study the current distribution at these resonances. In the structure of Fig. 2 the ground plane window used in Ref. 16 was suppressed. However, it is known that this fact does not substantially affect the response of the SRRs,[17] nor its current distribution (this last fact has been tested by specific simulations). The elimination of the ground plane window allows for the suppression of the spurious resonances due to the window itself,

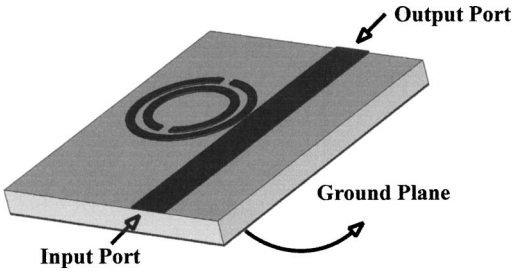

FIG. 2. Three-dimensional representation of a microstrip transmission line with an EC-SRR etched in the upper substrate side, close to the conductor strip.

which appear in addition to the SRR resonances when the window is present. Using this method, the resonant behavior of SRRs beyond the first (quasistatic) resonance is studied. Both EC-SRRs and NB-SRRs are considered, and the phenomenology associated with their different resonant modes will be compared and contrasted to the dynamic resonances appearing in single-ring resonators of identical dimensions. The simulations were carried out with the commercial software AGILENT MOMENTUM. This tool uses a frequency-domain algorithm, which is preferable to time-domain algorithms for the analysis of resonant structures. Moreover, the simulator allows us to monitor the fields and currents in the SRRs, this being of paramount importance in our study. The SRR resonances are identified from the transmission notches present in the transmission coefficient of such a microstrip line loaded with a single SRR.

Following the aforementioned method, the frequencies of resonance of a NB-SRR have been computed. The results for the transmission coefficient are shown in Fig. 3. In this figure, the frequencies of resonance of a single ring (identical to those that form the NB-SRR), computed by the same method, are also shown. It can be clearly observed that these last resonances are placed between the NB-SRR resonances, in agreement with the above theory. In Fig. 4, the frequencies of resonance of an EC-SRR of dimensions similar to those of the previous NB-SRR, are shown. The frequencies of resonance of the individual rings forming the EC-SRR are also shown in the figure. It is worth mentioning that the frequency

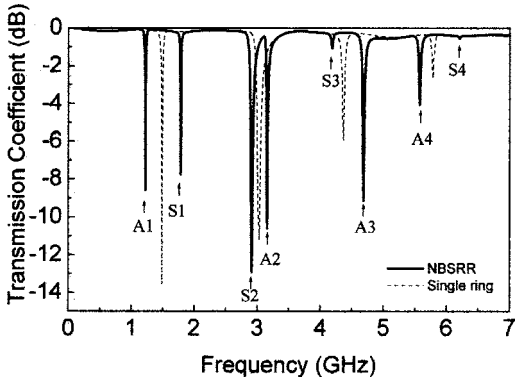

FIG. 3. Computed frequency response for a microstrip transmission line loaded with a NB-SRR. r_{ext}=6.217 mm, c=0.56 mm, d=0.37 mm, and g =0.6 mm. The substrate parameters are thickness h=0.49 mm and dielectric constant ε_r=2.43, i.e., those corresponding to the commercial Arlon 250-LX0193-43-11 microwave substrate.

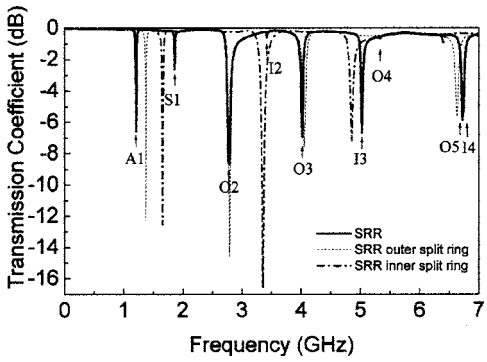

FIG. 4. Computed frequency response for a microstrip transmission line loaded with an EC-SRR. r_{ext}=6.217 mm, c=0.56 mm, d=0.37 mm, and g =0.6 mm. The substrate parameters are identical to those of Fig. 3.

for the first resonance is identical for both the EC-and the NB-SRR, as is expected from a previous analysis.[12] The first and the second EC-SRRs resonances seem to follow a similar schema that for the NB-SRR resonances. However, as it is expected from the theory proposed in Sec. II, the remaining EC-SRR resonances do not follow the same pattern that for the NB-SRR resonances.

To gain more insight on this complex phenomenology, we have also obtained the currents induced in the rings at the different resonant frequencies. These are depicted in Fig. 5 for the NB-SRR analyzed in Fig. 3. The average current intensity is shown in the second column of the figure, and the relative direction of the current flow at the maximum intensity points is shown in the third column. The currents clearly show an antisymmetric or a symmetric pattern, which agrees to the previous theory. Therefore, the resonances are labeled as A1, A2,… and as S1, S2,… . In this classification, the numeric character indicates the number of current maxima and the capital letter the symmetry of the currents. It is interesting to mention that the symmetric and antisymmetric resonant modes for the NB-SRR do not always alternate. Indeed, changes in the alternance occur for the even-order resonances (S2, A2, S4, A4,…). For these resonances, currents are maximized in the same regions for both rings, and the lower resonant frequency is that corresponding to currents flowing in the same direction. For the third resonance (S2), currents are symmetric; however, for the seventh resonant mode (A4), currents are clearly antisymmetric. In both cases, the rings currents are parallel. For the even-order modes, an explanation to the fact that the first resonance is that corresponding to parallel current flow can be found in an analogy with the propagation of the even modes in parallel coupled lines. The propagation velocity for these modes is higher than for the odd modes (which are the equivalent of resonances with antiparallel current flow) and hence the resonant frequency is lower.

The current patterns for the resonances of the EC-SRR of Fig. 4 are shown in Fig. 6. As it was already mentioned, these patterns approximately follow the antisymmetric-symmetric nature for the first two resonances. However, beyond the third-order resonance, current patterns substantially differ from those of the NB-SRR. As it was already mentioned, this fact can be expected from the lack of inversion

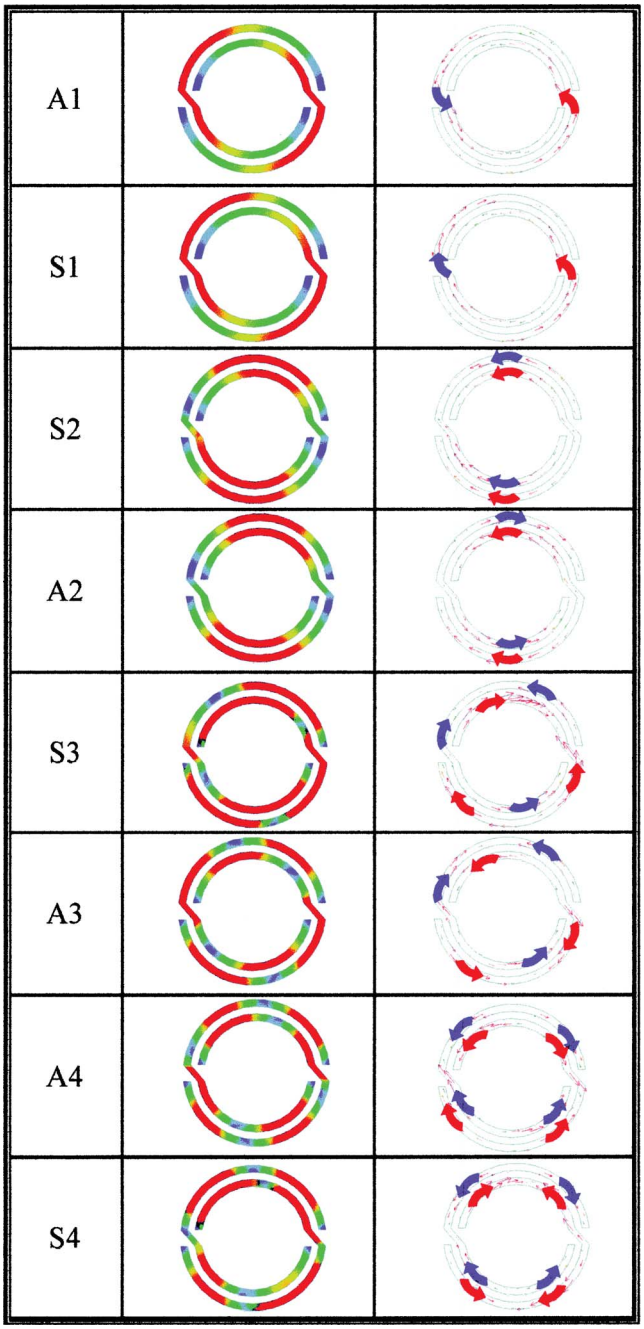

FIG. 5. (Color) Results of simulation of the induced currents in the NB-SRR of Fig. 3 at the different resonant frequencies, obtained by edge excitation (see Fig. 2). Both the intensity and direction of current flow are indicated.

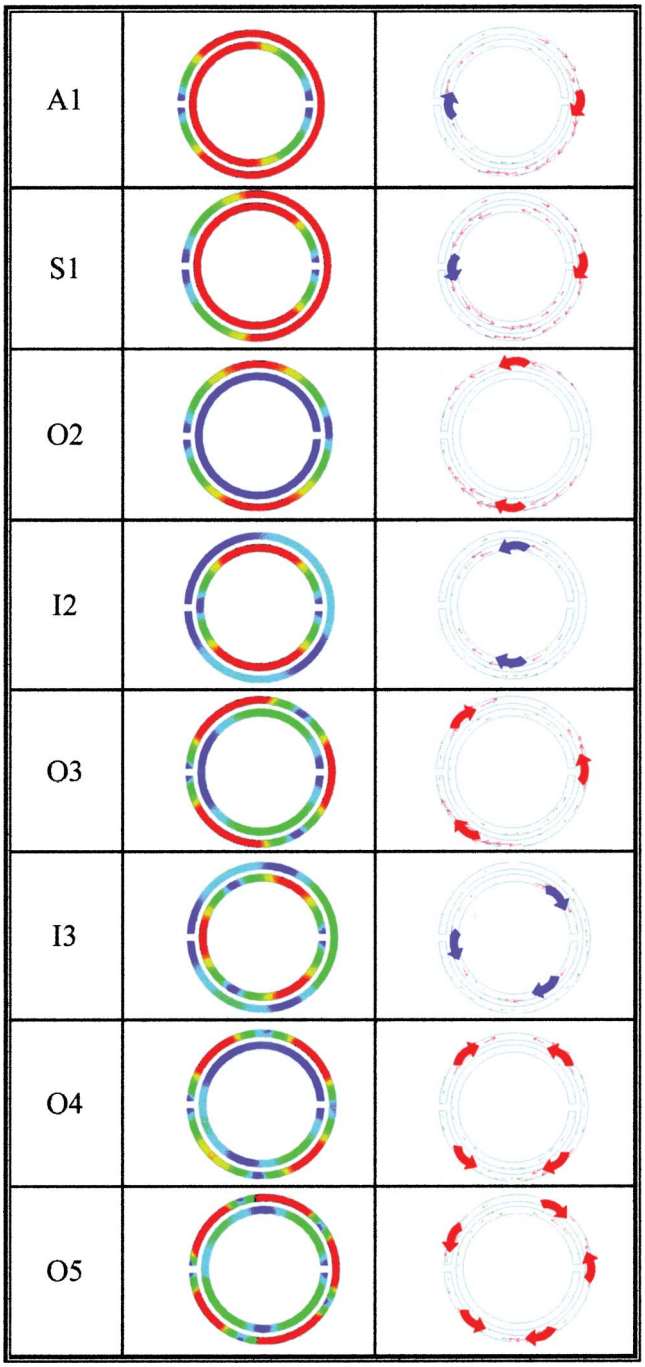

FIG. 6. (Color) Results of simulation of the induced currents in the EC-SRR of Fig. 4 at the different resonant frequencies, obtained by edge excitation (see Fig. 2). Both the intensity and direction of current flow are indicated.

symmetry of the EC-SRR. Indeed, the current patterns for these higher-order resonances clearly suggest that there is a single ring which is mainly excited. This fact is consistent with the proximity of these resonances to those of single rings, as it is shown in Fig. 4. Therefore the third and higher resonances were labeled as O2, O3,… and I2, I3,… . In this classification, the numeric character indicates the number of current maxima and the capital letter the ring (outer or inner) which is mainly excited. As a general conclusion of this paragraph, it can be said that the lower-order resonances of an EC-SRR approximately follow the same antisymmetric-symmetric pattern as those of the NB-SRR. However, this schema is not applicable to EC-SRR higher-order resonances, which mainly correspond to the excitation of a single (the inner or the outer) ring.

The resonance properties of BC-SRR are not analyzed in this section (they will be analyzed in Sec. IV). However, it can be expected that they will follow a similar schema as for the NB-SRR resonances. This is so because this particle, like the NB-SRR, exhibits inversion symmetry and hence nonbi-anisotropy. To summarize, in this section we have analyzed the nature of the different resonances exhibited by the different SRR configurations. For the NB-SRR and BC-SRR these resonances can be classified according to the symmetry or

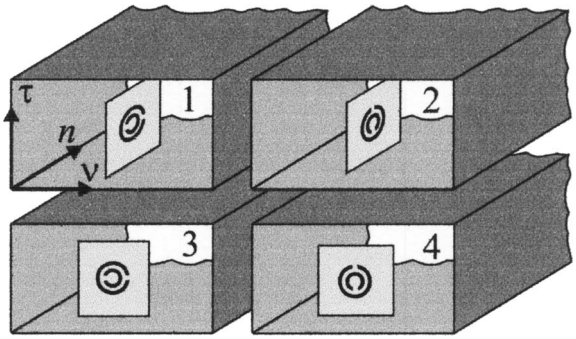

FIG. 7. Different orientations of the SRR inside the waveguide which allow to excite the resonances magnetically or electrically, or in both ways at the same time. The figure also holds for the NB-SRR and BC-SRR, provided they are oriented as is shown in Fig. 1.

antisymmetry of ring currents. For the EC-SRR this classification is not appropriate, although it still holds for the lower-order resonances. Higher-order EC-SRR resonances usually correspond to the excitation of a single ring.

IV. BEHAVIOR OF THE SRRS UNDER HOMOGENEOUS FIELD EXCITATION

To gain further insight on the resonance properties of the particles considered in this work, we have carried out both simulations and measurements on hollow metallic waveguides loaded with different resonator types and orientations. The advantage of waveguides over planar propagating media (such as a microstrip line) is the quasiuniformity of the excitation fields at the particle scale when the waveguide is excited in its fundamental mode. Therefore, waveguide excitation is specially well suited for the analysis of the SRR polarizabilities [see Eq. (1)], which are of interest in the homogenization of microstructured composites of these particles. The main disadvantage of waveguide excitation is that it is only feasible for the lower-order SRR resonances, because at higher-order resonant frequencies higher-order waveguide modes are also excited. For this reason microstrip excitation was used for the analysis of higher-order SRR resonances in Sec. III. We would like to mention that a numerical analysis of the first two resonances in SRRs (under different orientations) has been recently carried out by Kafesaki *et al.*[18] In the present work, we extend the analysis to NB-SRR as well as BC-SRRs, we give an explanation of the excited resonances in terms of the polarizabilities of the particles, and we provide experimental results to confirm the validity of the simulations, as will be shown in the following paragraphs.

For the aforementioned purpose the SRRs were located in the middle point of the waveguide, at the four orientations shown in Fig. 7. The excitation field is the fundamental TE_{10} waveguide mode, for which only the E_τ, B_ν, and B_n field components (see Fig. 7) are present, being $B_n=0$ at the location of the SRRs. Thus, in orientations (1) and (2) the resonator is excited by the electric (E_τ) and magnetic (B_ν) fields, whereas in positions (3) and (4), the excitation can be only due to the electric field (E_τ). Therefore, regarding Eq. (1), the five polarizabilities α_{yy}^{ee}, α_{xy}^{ee}, α_{yz}^{em}, α_{xz}^{em}, and α_{zz}^{mm} are relevant in position (1). In position (2) the relevant polarizabilities [with regard to the particle axis orientation as it is assumed in Eq. (1) and shown in Fig. 1] are α_{xx}^{ee}, α_{xy}^{ee}, α_{yz}^{em}, α_{xz}^{em}, and α_{zz}^{mm}. In position (3) the relevant polarizibilities are α_{yy}^{ee}, α_{xy}^{ee}, and α_{yz}^{em}, since there is no magnetic flux perpendicular to the particle, and no electric field along the x axis of the particle (see Fig. 1). Finally, for the same reasons, the relevant polarizabilities in position (4) are α_{xx}^{ee}, α_{xy}^{ee}, and α_{xz}^{em}.

The transmission coefficients through the different configurations of Fig. 7 are shown in Fig. 8, for frequencies near the first and second resonances of an EC-SRR [Figs. 8(a) and 8(b)], a NB-SRR [Figs. 8(c) and 8(d)], and a BC-SRR [Figs. 8(e) and 8(f)]. To begin with the BC-SRR in its first resonance [Fig. 8(e)], it can be observed that the BC-SRR is not excited in positions (3) and (4). That is, the polarizabilities α_{yy}^{ee}, α_{xy}^{ee}, α_{xx}^{ee}, α_{yz}^{em}, and α_{xz}^{em} vanish for this resonance. However, the particle is excited in orientations (1) and (2). That is, the polarizability α_{zz}^{mm} does not vanish (in fact it is the only nonvanishing polarizability at this resonance). Therefore, the first BC-SRR resonance is a *magnetic-type* resonance, in which only a magnetic dipolar moment is excited when the particle is placed in a homogeneous (at the particle scale) magnetic field. Regarding now to the second resonance of the BC-SRR [Fig. 8(f)], it can be deduced by a similar procedure that the only nonvanishing polarizability at this resonance is the α_{yy}^{ee} one. That is, the second BC-SRR resonance is an *electric-type* resonance which can be only excited (under homogeneous field excitation) by an electric field parallel to the y axis of the BC-SRR. At this point it is worth mentioning that the aforementioned results only deal with the strong *resonant* polarizabilities associated with the resonances. For physical reasons, all the SRRs analyzed in this paper must show some weak and nonresonant values for the α_{yy}^{ee} and α_{xx}^{ee} polarizabilities, which produce the small level of reflection in the waveguide present at all frequencies that can be seen in Fig. 8. Thus, and taking this last remark into account, all the reported experiments are in agreement with the theory reported in the preceding sections. In particular, they can be deduced from the antisymmetric (symmetric) nature of the first (the second) BC-SRR resonance.

The behavior of the NB-SRR under homogeneous field excitation at the first and the second resonances is analyzed in Figs. 8(c) and 8(d). The behavior of the NB-SRR at the first resonance [Fig. 8(c)] is completely similar to that of the BC-SRR, therefore we can conclude that this is a magnetic-type resonance, which can be only excited by a uniform magnetic B_z field, producing a magnetic dipolar moment m_z (see Fig. 1 for axis orientation). The behavior of the NB-SRR at the second resonance [Fig. 8(d)] is also quite similar to that of the NB-SRR. However, a small excitation is found for (2) and (4) orientations. We interpret this result as a consequence of a small but nonvanishing resonant values for the α_{xy}^{ee} and α_{xx}^{ee} polarizabilities. As it was mentioned in Sec. II, this fact is expected from the lack of reflection symmetry of the NB-SRR with regard to the x-z plane (see Fig. 1). Thus, except for this small difference, the behavior of the NB-SRR is quite similar to that of the BC-SRR. In particular, the second NB-SRR resonance is also an electric-type resonance, which can be only excited by uniform electric fields.

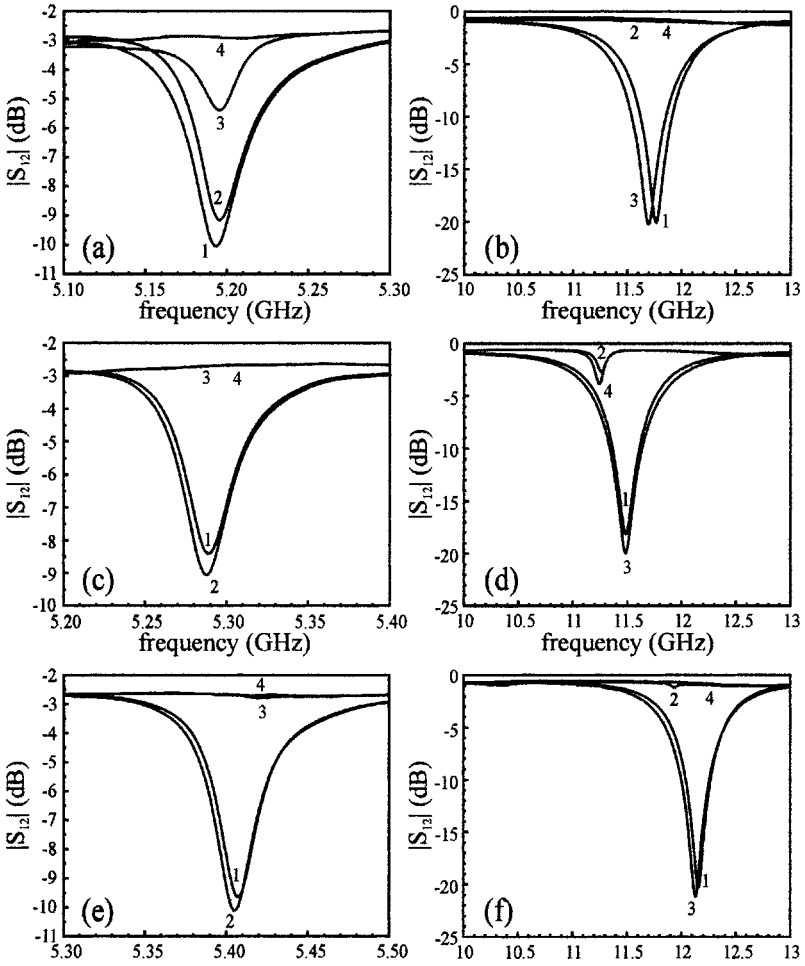

FIG. 8. Measurements of first-order (first column) and second-order (second column) resonances for EC-SRR, NBSRR, and BCSRR (first, second, and third row, respectively). The numbers close to the curves indicate the different orientations shown in Fig. 7. The resonators are printed on a substrate with thickness $t=0.49$ mm and relative permittivity $\varepsilon_r=2.43$. The parameters of EC-SRR and NB-SRR, named just as in Fig. 1, are $r_{\text{ext}}=2.53$ mm, $c=0.16$ mm, $d=0.19$ mm, and $g=0.26$ mm. These parameters lead to a theoretical first resonance frequency 5.14 GHz. In the BC-SRR case, $r_{\text{ext}}=2.28$ mm, $c=0.5$ mm, $g=0.5$ mm, and the first resonance occurs at 5.27 GHz. For the first (quasistatic) resonance measurements a WR137 rectangular waveguide with a 35×16-mm^2 cross section was used. For the second resonance a WR90 rectangular waveguide with a 23×10-mm^2 cross section was used.

The behavior of the EC-SRR at its first [Fig. 8(a)] and second resonances [Fig. 8(b)] is quite different from that of the BC-SRR and the NB-SRR. For the first resonance [Fig. 8(a)] we can only deduce that the polarizabilities α_{xx}^{ee}, α_{xy}^{ee}, and α_{xz}^{em} do not take resonant values at this resonance [see the curve for orientation (4)]. Previous analysis of this resonance[9,13] have predicted that the α_{xz}^{em} polarizability must vanish, and that the α_{yz}^{em} one is nonzero. Thus, these analyses are consistent with the results shown in Fig. 8(a). It is worth mentioning that the main particle excitation occurs at orientation (1), where all the resonant polarizabilities α_{yy}^{ee}, α_{yz}^{em}, α_{zz}^{mm} are in operation. The lower excitation level occurs in orientation (3), for which only the electric field is exciting the particle. Therefore, the first EC-SRR resonance can be characterized as a magnetoelectric resonance, which can be excited by both electric and magnetic uniform fields with the appropriate polarization, generating both electric and magnetic dipolar moments, and being the electric excitation weaker than the magnetic one. All these results are in agreement with the previous analysis.[9,13] The second EC-SRR resonance [Fig. 8(b)] shows a quite different behavior. In fact, this behavior is completely similar to that of the second BC-SRR resonance [Fig. 8(f)]. Therefore, it is deduced that this resonance is an electric-type resonance (rather than magnetoelectric), which is excited by a uniform E_y field, producing an electric resonant dipole in this direction. It is worth mentioning that from the symmetries of the EC-SRR, the second resonance might exhibit magnetoelectric coupling, however, this is not present, thus being a quite surprising result. We will return to this point in the next paragraph.

The fundamental mode of the considered rectangular waveguide is a TE mode, with some variations of the electromagnetic field across the waveguide section. Thus, in fact, we have analyzed the behavior of the SRRs under quasiuniform field excitation, not under strictly uniform field excitation. To do that, we would need a transmission electron microscopy (TEM) mode. However, these modes do not propagate in metallic waveguides. Nevertheless, we can numerically simulate such modes by replacing the lateral sidewalls of the waveguide shown in Fig. 7 by *perfect magnetic conductors*. These simulations (not shown in this paper), carried out by using the commercial CST MICROWAVE STUDIO electromagnetic solver, confirm the experimental results reported in this section. In particular, they have confirmed that the second EC-SRR resonance is only excited by the electric field. This conclusion is illustrated in Fig. 9, where the behavior of two different EC-SRRs excited at the second resonance inside a TEM waveguide has been simulated.

V. CONCLUSIONS

The resonant properties of EC-SRRs, NB-SRRs, and BC-SRRs have been analyzed. Similarities between the NB-SRR and the BC-SRR have been found due to the similar

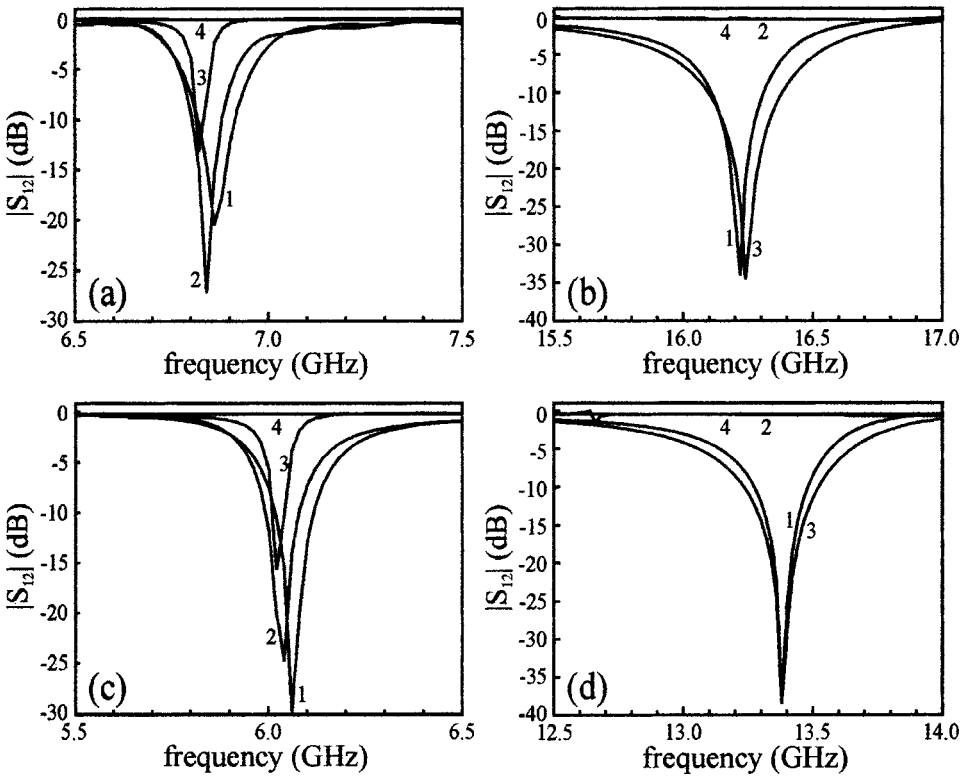

FIG. 9. Simulation of the transmission coefficient in the vicinity of the first two resonances for two EC-SRR-loaded TEM waveguides. The EC-SRR dimensions are $r_{ext}=2.6$ mm, $c=0.5$ mm, and $d=0.2$ mm [(a) and (b)]; and $r_{ext}=3$ mm, $c=0.5$ mm, and $d=0.3$ mm [(b) and (c)].

symmetry properties of both particles, whereas the phenomenology associated with the EC-SRR is more complex due to the bianisotropic behavior of this resonator. The analysis of the currents induced in these particles has revealed that for the first-order resonances both rings are excited, being the first (quasistatic) resonance classified as antisymmetric while the second as symmetric. For higher-order resonances, a different behavior has been obtained for the EC-SRR and NB-SRR. While for the NB-SRR it has been found that both rings are excited and the resonances can be also classified in terms of symmetric or antisymmetric, for the EC-SRR, we have found that only one (the inner or the outer) ring is excited, and the resonance frequency coincides to a good approximation to that corresponding to a single ring with an aperture (slit) and identical dimensions. Obviously, in this case, the classification of higher-order resonances as symmetric or antisymmetric is no longer valid and resonances can be identified by simply indicating the order (number of current maxima) and the ring where currents have been induced. For the NB-SRR (and BC-SRRs) antisymmetric resonances have been associated with the presence of a nonzero magnetic moment, while a dipolar electric moment is present in the resonances classified as symmetric. By embedding the resonators under study in a rectangular metallic waveguide, it has been found that the lower-order (the first and the second ones) resonances for NB-SRRs and BC-SRRs can be either magnetically (quasistatic resonance) or electrically (symmetric mode) excited, and this selective excitation has been attributed to the lack of cross-polarization effects, that is related to the inversion symmetry that the particles exhibit. However, for the EC-SRRs cross-polarization effects are present, with the result of both magnetic and electric excitations for the quasistatic resonance. However, only electric excitation has been observed for the second resonance. This behavior has been attributed to the lack of magnetic moment for the second resonance and has been corroborated by multiple simulations of TEM waveguides loaded with different EC-SRRs. The main contribution of this work is the comprehensive analysis and classification of the resonances and polarizabilities in bianisotropic (EC-SRRs) and nonbianisotropic (including NB-SRRs and BC-SRRs) SRRs. This analysis has been supported by experiments (in a waveguide environment) and simulations (of microstrip and TEM waveguide excitations).

ACKNOWLEDGMENTS

This work has been supported by MEC (Spain) by project Contract Nos. TEC2004-04249-C02-01 and TEC2004-04249-C02-02 and by the European Community (Eureka program) by Project No. 2895 TELEMAC. This work has been also supported by the Grant Agency of the Czech Republic under Project No. 102/03/0449.

[1] J. B. Pendry, A. J. Holden, D. J. Robbins, and W. J. Stewart, IEEE Trans. Microwave Theory Tech. **47**, 2075 (1999).
[2] D. R. Smith, W. J. Padilla, D. C. Vier, S. C. Nemat-Nasser, and S. Schultz, Phys. Rev. Lett. **84**, 4184 (2000).
[3] V. G. Veselago, Sov. Phys. Usp. **10**, 509 (1968).
[4] R. A. Shelby, D. R. Smith, and S. Schultz, Science **292**, 77 (2001).
[5] R. Marqués, J. Martel, F. Mesa, and F. Medina, Phys. Rev. Lett. **89**, 183901 (2002).
[6] S. Hrabar and J. Bartolic, Proceedings of the ICECOM'2003, Dubrovnik, Croatia, 2003 (unpublished), p. 51.
[7] F. Martín, F. Falcone, J. Bonache, R. Marqués, and M. Sorolla, Appl. Phys. Lett. **83**, 4652 (2003).
[8] F. Falcone, F. Martín, J. Bonache, R. Marqués, T. Lopetegi, and M. Sorolla, IEEE Microw. Wirel. Compon. Lett. **14**, 10 (2004).
[9] R. Marqués, F. Medina, and R. Rafii-El-Idrissi, Phys. Rev. B **65**, 144440 (2002).

[10]F. Falcone, F. Martin, J. Bonache, R. Marqués, and M. Sorolla, Microwave Opt. Technol. Lett. **40**, 3 (2004).
[11]P. Gay-Balmaz and O. J. F. Martín, J. Appl. Phys. **92**, 2929 (2002).
[12]R. Marqués, J. D. Baena, J. Martel, F. Medina, F. Falcone, M. Sorolla, and F. Martín, Proceedings of the International Conference in Electromagnetics for Advanced Applications (ICEAA'03), Torino, Italy, 2003 (unpublished), p. 439.
[13]R. Marqués, F. Mesa, J. Martel, and F. Medina, IEEE Trans. Antennas Propag. **51**, 2572 (2003).
[14]M. Shamonin, E. Shamonina, V. Kalinin, and L. Solymar, Microwave Opt. Technol. Lett. **44**, 133 (2005).
[15]L. Landau and E. Lifshitz, *Statistical Physics*, 3rd ed. (Pergamon, Oxford, 1984).
[16]J. D. Baena, R. Marqués, F. Medina, and J. Martel, Phys. Rev. B **69**, 014402 (2004).
[17]J. García-García *et al.*, Microwave Opt. Technol. Lett. **44**, 376 (2005).
[18]M. Kafesaki, T. Koschny, R. S. Penciu, T. F. Gundogdu, E. N. Economou, and C. M. Sokoulis, J. Opt. A, Pure Appl. Opt. **7**, S12 (2005).